Inorganic Chemistry
Article

Inorg. Chem. **2010**, *49*, 4099–4108 **4099**
DOI: 10.1021/ic902076r

Molecular, Electronic, and Crystal Structures of Self-Assembled Hydrothermally Synthesized Zn(II)−Mercaptonicotinate: A Combined Spectroscopic and Theoretical Approach

Maurizio Casarin,[†] Thomas Devic,[‡] Alessia Famengo,[†] Daniel Forrer,[†] Silvia Gross,*[,†] Eugenio Tondello,[†] and Andrea Vittadini[†]

[†]*Istituto di Scienze e Tecnologie Molecolari, ISTM-CNR and Dipartimento di Scienze Chimiche, Università degli Studi di Padova, via Marzolo, 1, I-35131, Padova, Italy and INSTM, UdR Padova, and* [‡]*Institut Lavoisier, UMR CNRS 8180, Université de Versailles Saint-Quentin-en-Yvelines, 45 Avenue des Etats-Unis, 78035 Versailles, France*

Received October 21, 2009

A Zn(II) 2-mercaptonicotinate coordination polymer (**Zn1**), with Zn(II) ions chelated by both sulfur and oxygen in a distorted square pyramidal environment, and a molecular Zn(II) 2-hydroxynicotinate complex (**Zn2**) were synthesized by the reaction of zinc acetylacetonate with 2-mercaptonicotinic (**Zn1**) and 2-hydroxynicotinc (**Zn2**) acid, respectively, under hydrothermal conditions. The crystal structures of **Zn1** and **Zn2** were determined by single crystal X-ray diffraction measurements. Dispersion-corrected density functional theory (DFT) calculations reproduce very well the experimental structures and show that **Zn1** is stable against hydration, whereas **Zn2** is stable against dehydration over wide ranges of temperature and pressure, in agreement with thermogravimetric analysis results. The electronic structure of the two compounds is computed with the DFT+U method. The theoretical valence band agrees well with the X-ray photoelectron spectroscopy experiments. Furthermore, the band gap of **Zn1** is found to be narrower than that of **Zn1** and is characterized by the presence of sulfur lone pairs at the edge of the valence band.

Introduction

The molecular engineering of transition-metal-based coordination compounds and extended networks is a rapidly growing area of research, not only for the fundamental chemical and topological issues triggered by these self-assembled systems[1] but also for their functional properties and potential applications.[2] In this habit, the use of heteronuclear polydentate and polynucleating ligands is of particular interest because they can lead to the formation of extended systems with unusual electronic and optical properties.[3,4]

Compared to the vast literature on the synthesis of coordination polymers and metal−organic frameworks (MOFs) based on N- and O-coordinating ligands,[3a,5] reports focusing on complexes of bifunctional S- and O-donors are rather scarce.[6] This latter class of ligands is particularly interesting because they are in principle able to accomplish new topologies and coordination fashions, with still unexplored electronic and optical properties. In this respect, it has to be mentioned that even if many examples of bridging S−M−O bonds are reported in literature, most of them imply a bidentate *bridging* coordinative mode.[7] Much more interesting is the formation of heteroleptic complexes with S and O

*Corresponding author. E-mail: silvia.gross@unipd.it.

(1) (a) Kitagawa, S.; Noro, S. *Compr. Coord. Chem. II* **2004**, *7*, 231. (b) Hong, M. *Cryst. Growth Des.* **2007**, *7*, 10. (c) Batten, S. R.; Robson, R. *Angew. Chem., Int. Ed.* **1998**, *37*, 1460. (d) Zaworotko, M. J. *Chem. Commun.* **2001**, *37*, 1.

(2) (a) Kitagawa, S.; Kitaura, R.; Noro, S. *Angew. Chem., Int. Ed.* **2004**, *43*, 2334. (b) Maspoch, D.; Ruiz-Molina, D.; Veciana, J. *J. Mat. Chem.* **2004**, *14*, 2713. (c) Janiak, C. *Dalton Trans.* **2003**, 2781. (d) Chen, T.-C.; Chin; Suslick, K. S. *Coord. Chem. Rev.* **1993**, *128*, 293. (e) Ferey, G. *Dalton Trans.* **2009**, *23*, 4400–4415. (f) Ferey, G. *Stud. Surf. Sci. Catal.* **2007**, *168*, 327–374. (g) Ferey, G. *Chem. Soc. Rev.* **2008**, *37*, 191–214. (h) Guillou, N.; Livage, C.; Ferey, G. *Eur. J. Inorg. Chem.* **2006**, *24*, 4963–4978. (i) Mellot-Draznieks, C.; Girard, S.; Ferey, G.; Schon, J. C.; Cancarevic, Z.; Jansen, M. *Chem.—Eur. J.* **2002**, *8*, 4102–4113. (j) Ferey, G. *J. Solid State Chem.* **2000**, *152*, 37–48. (k) Ferey, G. *Stud. Surf. Sci. Catal.* **2007**, *170A*, 66–86. (l) Ferey, G. *J. Solid State Chem.* **2000**, *152*, 37–48.

(3) (a) Thematic Issue on MOF in *Chem. Soc. Rev.* **2009**, *38*, and references therein. (b) Zyss, J. *Molecular Non-Linear Optics: Materials, Physics and Devices*, Academic Press: New York, NY, 1993.

(4) Lin, W.; Evans, O. R.; Xiong, R.-G.; Wang, Z. *J. Am. Chem. Soc.* **1998**, *120*, 13272.

(5) (a) Robin, A. Y.; Fromm, K. M. *Coord. Chem. Rev.* **2006**, *250*, 2127. (b) Zhou, Y.; Hong, M.; Wu, X. *Chem. Comm.* **2006**, *135*. (c) Erxleben, A. *Coord. Chem. Rev.* **2003**, *246*, 203. (d) Na X., Wei, S., Dai-Zheng, L., Shi-Ping, Y., Peng, C. *Inorg. Chem.* **2008**, *47*, 8748−8756.

(6) (a) Goodman, D. C.; Farmer, P. J.; Darensbourg, M. Y.; Reibenspies, H. J. *Inorg. Chem.* **1996**, *35*, 4989. (b) Khandwe, M.; Bajpai, A.; Bajpai, U. D. N. *Polym. Bull.* **1990**, *23*, 51.

(7) (a) Wang, Y.; Zhu, D.-H.; Su, Z.-M.; Shao, K.-Z.; Zhao, Y.-H. *Acta Crystallogr., Sect. C: Cryst. Struct. Commun.* **2008**, *C64*, m70. (b) Humphrey, S. M.; Mole, R. A.; Rawson, J. M.; Wood, P. T. *Dalton Trans.* **2004**, 1670. (c) Cindric, M.; Strukan, N.; Kajtez, T.; Kamenar, B.; Geister, G. *Z. Anorg. Allg. Chem.* **2001**, *627*, 2604. (d) Toma, M.; Sanchez, A.; Garcia-T.; Maria, S.; Casas, J. S.; Sordo, J.; Castellano, E. E.; Ellena, J. *Cent. Eur. J. Chem.* **2004**, *2*, 534–552.

Published on Web 03/31/2010

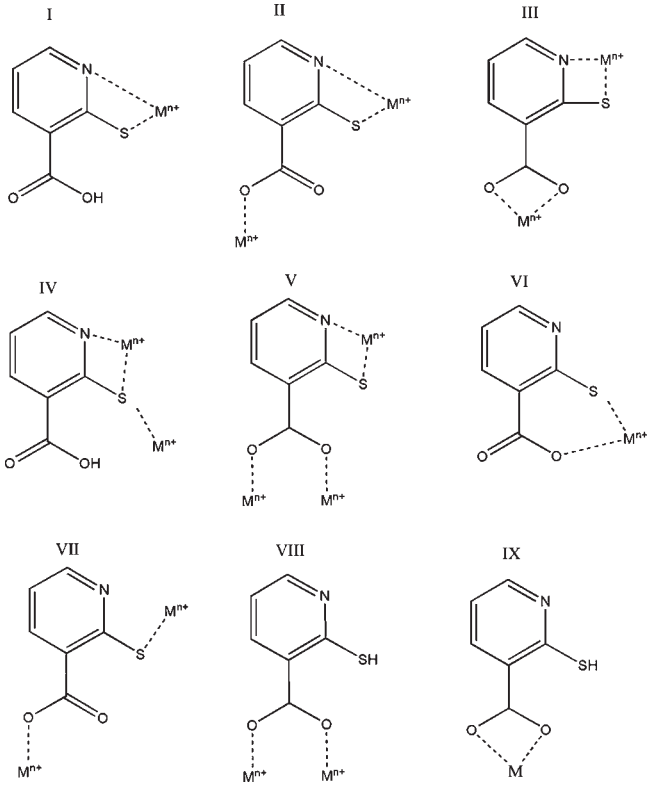

Figure 1. Different coordination modes for 2-mercaptonicotinic acid.

atoms *chelating* the same metal ion, since the S−M−O fragment is expected to be characterized by electronic properties significantly different from those of the O−M−O one. This particular typology of coordination can be achieved either by using thiocarboxylic acid (e.g., thioacetic acid) or by resorting to bifunctional thiolate−carboxylate ligand, such as mercapto carboxylic acids.

In S,O polytopic ligands, the additional presence of nitrogen donor atoms further widens the coordination possibilities, since different donor sites (S, O, N) compete in the coordination to the metal ion and different coordination fashions can be observed, also according to the nature of the metal. This variability in terms of coordination modality affects the electronic properties of the final complex as well.

In this study, the synthesis and the characterization of a new Zn coordination compounds by using 2-mercaptonicotinic acid is reported (**Zn1**). For comparison, the same experimental conditions used for the 2-mercaptonicotinic acid were also applied to the oxygen homologue, 2-hydroxynicotinic acid. In this case, the complex **Zn2**, displaying the same coordination mode as **Zn1** was obtained, which, however, has a different coordination geometry around the Zn atom and a different supramolecular arrangement.

These organothiolato carboxylates offer the possibility of variable coordination and chelation modes toward metal ions; some of the most common examples of these modes are shown in Figure 1.

As far as the first basic issue is concerned, our main aim was that of exploiting the coordination possibilities of the chosen ligands, their supramolecular arrangement and how the metal (in this case zinc) tends to coordinate to a sulfur donor site if other chelation modes (to nitrogen or to the carboxylate) are available. Also, as pointed out in previous works,[5] in many cases rather similar ligands lead to completely different coordination arrays, and the understanding of the structure-determining factors is of fundamental importance in coordination polymer chemistry.

Several Zn(II)-based coordination polymers are known and characterized.[5,7−10] The d^{10} metal ion Zn^{2+} is particularly prone to form coordination polymers, since it can display coordination geometries different from the usual tetrahedral one, such as the octahedral, trigonal planar, trigonal pyramidal, and square pyramidal.[8] Nicotinic acid has been already used as bi- and tridentate-bridging unit for the preparation of three-dimensional (3D) Zn- and Cd-based coordination polymers,[4,9] whereas the formation of two isomorphous interpenetrating 2D frameworks of Cu and Zn by using a mixture of nicotinic and isonicotinic ligands has been reported by Li et al.[10]

In the present work, we switch to the mercapto derivative to explore the possibility of achieving formation of mixed S−M−O bonds, with the aim of exploiting the sulfur species to tune the electronic properties of the complex. The proposed ligand has different potential coordinative modes,[7b] as depicted in Figure 1: (i) S-,N-donor chelate and carboxylic group uncoordinated;[7b,c] (ii) S-,N-donor chelate and carboxylic group in monodentate coordination mode;[7d] (iii) S-,N-donor chelate and carboxylic group in O,O-chelating mode;[7a,d] (iv) S−N donor chelate, S-donor mode, and non-coordinated carboxylic group;[7d] (v) S-,N-donor chelate and carboxylic group in multidentate-bridging coordination mode;[7d] (vi) S-,O-chelating mode and not coordinated nitrogen atom (the **Zn1** coordinative mode); (vii) S-,O-bridging mode and non-coordinated nitrogen atom;[7a,d] and finally (viii−ix) O-,O-bridging and O-,O-chelating modes with non-coordinated S,N.[7b]

We point out that the structure peculiarity of the 2-mercaptonicotinic isomer, with thiolate and carboxylate groups in α and β position with respect to the pyridinic nitrogen, plays a key role in determining the final structure. In fact, the close ortho proximity of the two coordinating groups favors the formation of the heteroleptic compound with the two S and O atoms coordinating the same Zn^{2+} ion. A similar effect, in that case involving two O atoms (from carboxylate and hydroxy group), was observed in the case of the hydroxynicotinic acid.

A further and related point we aimed at investigating in this study was the electronic structure of the S,O compound as compared to the O,O homologue. To this aim, the obtained crystal structures were used as starting points for periodic density functional theory (DFT) calculations to determine the electronic structure of the compounds.

From a synthetic point of view, a final goal of this work was to synthesize molecular building blocks which could be potentially used as single source precursors for the synthesis of ZnO_xS_{1-x} ($0 < x < 1$) nanostructures.

(8) Holleman, A. F.; Wiberg, E. *Lerhrbuch der Anorganischen Chemie*, 101st ed.; W. De Gruyter: Berlin, Germany, 1995

(9) (a) Chen, H.-J. *Acta Crystallogr.* **2005**, *E61*, m616. (b) Lu, J.; Zhao, K.; Fang, Q.-R.; Xu, J.-Q.; Yu, J.-H.; Zhang, X.; Bie, H.-Y.; Wang, T.-G. *Cryst. Growth Des.* **2005**, *5*, 1091. (c) Abu-Youssef, M. A. M. *Polyhedron* **2005**, *24*, 1829.

(10) Li, F.; Wang, Y.; Li, G.; Sun, Y.; Gu, X.; Gao, E. *Inorg. Chem. Commun.* **2007**, *10*, 767.

Experimental Section

Chemicals. $Zn(acac)_2$ (bis-2,4-pentanedionate zinc, $Zn(CH_3COCHCOCH_3)_2 \cdot xH_2O$), 2-mercaptonicotinic, and 2-hydroxynicotinc were purchased by Aldrich, Milan, Italy.

Synthesis of $Zn(C_6H_4NO_2S)_2$ (Zn1). The **Zn1** complex was hydrothermally synthesized (autogenous pressure) from a mixture of 0.15 g (0.57 mmol) of zinc acetylacetonate, (bis-2,4 pentanedionate zinc, $Zn(CH_3COCHCOCH_3)_2 \cdot xH_2O$ Aldrich) and 5 equiv (0.44 g, 2.84 mmol) of 2-mercaptonicotinic acid ($C_6H_6NO_2S$, Aldrich, 97%) in 13 mL of water. The reactants were stirred a few minutes at room temperature (RT) before pouring the resulting suspension in a Teflon lined stainless steel autoclave and treating at 373 K for 96 h. Eventually, a further heating at 423 K for 5 h was carried out. The autoclave was left cooling at RT. The yellow solid was filtered and washed several times with ethanol, water and finally with acetone. Needle-shaped crystals were recovered which were suitable for X-ray single crystal analysis.

Synthesis of $Zn(C_6H_4NO_3)_2(H_2O)_2$ (Zn2). The **Zn2** complex was hydrothermally synthesized (autogenous pressure) in the same conditions used for **Zn1** but using 2-hydroxynicotinic acid, instead of 2-mercaptonicotinic acid.

Elemental Analysis (Calculated) for $Zn(C_6H_4NO_2S)_2$. Found (calcd): C: 37.80 (38.60), H: 2.13 (2.11), N: 7.44 (7.50), S:17.40 (17.10).

Elemental Analysis (Calculated) for $Zn(C_6H_4NO_3)_2(H_2O)_2$. Found (calcd): C: 38.47 (38.34), H: 3.38 (3.22), N: 7.49 (7.46).

FT-IR Data of $Zn(C_6H_4NO_2S)_2$ (KBr, cm^{-1}). 3440 (broad, w; ν N−H) 3087 (w; δ C−H), 3074 (w; δ C−H), 1683 (vw), 1612 (m/s; ν_{asym} COO−), 1569 (s; δ N−H+ ν C═N), 1488 (m/s; ν_{sym} COO−); 1442 (m/w), 1421 (w); 1357 (m, ν C═N+ ν C═S), 1236 (s), 1139 (m, ν C═S),[11] 1081 (w), 1058 (w; ν C═N+ ν C═S), 1006 (m/w) 919 (w), 850 (w), 821(w), 777 (m), 752 (w; δ C−H), 709 (w; δ C−H), 642 (m; ν C═N+ ν C═S), 563 (w), 545 (w), 499 (m), 485 (m), 408 (m; ν Zn−O).[12]

FT-IR Data of $Zn(C_6H_4NO_3)_2(H_2O)_2$ (KBr, cm^{-1}). 3371 (m/w; ν N−H) 3200−2917 (broad; δ C−H, ν−OH H_2O), 1635 (s; ν_{asym} COO−), 1572, (m;(δ N−H+ ν C═N)), 1550 (m; ν_{sym} COO−), 1489 (w); 1461 (w), 1421(m), 1378 (m), 1317 (w), 1234 (s), 1151 (m), 1123 (m; ν C−O), 1089 (w), 1078 (m/w), 989 (w), 950 (w), 902 (m/s), 835 (w), 781 (m/s; δ C−H), 742 (w), 725 (w; δ C−H), 663 (w/m), 573 (m/s), 526 (m/s), 485 (m), 404 (m; ν Zn−O).[12]

Methods

FT-IR analysis. FT-IR experiments were performed with a NEXUS 870 FT-IR (NICOLET), operating in the trasmission range from 400 to 4000 cm^{-1}, collecting 64 scans with a spectral resolution of 4 cm^{-1}. The measurements were recorded by dispersing the crystals in anhydrous KBr. Anhydrous KBr was purchased by Merck GmbH, Darmstadt, Germany.

XPS analysis. The crystalline compounds **Zn1** and **Zn2** as well the 2-mercaptonicotinic acid were investigated by X-ray photoelectron spectroscopy (XPS) with a Perkin-Elmer Φ 5600ci instrument using standard Al−K_α radiation (1486.6 eV) operating at 350 W. The working pressure was $\leq 5 \times 10^{-8}$ Pa $\sim 10^{-11}$ Torr. The calibration was based on the binding energy (BE) of the Au4$f_{7/2}$ line at 83.9 eV with respect to the Fermi level. The standard deviation for the BE values was 0.15 eV. The reported BE's were corrected for the BE's charging effects, assigning the BE value of 284.6 eV to the C1s line of carbon.[13] Survey scans were obtained in the 0−1350 eV range (pass energy 187.5 eV, 1.0 eV/step, 50 ms/step). Detailed scans (58.7 eV pass energy, 0.1 eV/step, 100−150 ms/step) were recorded for the O1s, C1s, Zn2p, S2p, S2s, and ZnLMM regions. The atomic composition, after a Shirley-type background subtraction,[14] was evaluated using sensitivity factors supplied by Perkin-Elmer.[15] Charge effects were partially compensated by using a charge neutralizer (flood gun). Peak assignment was carried out according to literature data.[13,15,16] Valence bands were acquired in the −5−25 eV range (11.85 eV pass energy, 0.1 eV/step, 200 ms/step)

Elemental analysis. Elemental analyses were obtained in the Microanalysis Laboratory of the Department of Chemistry of the University of Padova by using a Frisons EA 1108 instrument.

Thermogravimetric analyses (TGA). TGA and differential scanning calorimetry (DSC) for **Zn1** and **Zn2** were performed in air or nitrogen atmosphere on a LabSys Setarm SDT 2960 instrument in the temperature range 29−800 °C, using a heating rate of 10 °C/min.

X-ray crystallography. Single crystals of **Zn1** and **Zn2** were mounted on a glass fiber and measured at RT on a Bruker-Siemens SMART CCD diffractometer equipped with a Mo anode and a graphite monochromator. The data reduction and absorption correction were performed with the SAINT and SADABS softwares, respectively. The structure was solved by direct methods and refined by full-matrix least-squares techniques, based on F^2, using the SHELX software package. All non-hydrogen atoms were refined anisotropically. Hydrogen atoms of the ligands were introduced at calculated positions and were not refined, whereas the ones of the water molecules in **Zn2** were found on the Fourier map, and their positions refined with constraints (O−H = 0.8 Å). Crystal data and refinement parameters are summarized in Table 1.

Computational Details. Theoretical calculations on the title compounds were carried out with the PWSCF code, which is part of the Quantum-ESPRESSO (QE) suite,[17] and it is a plane-wave pseudopotential implementation of the DFT. Because noncovalent interactions cannot be neglected in the examined systems, we have used the DFT-D approach by Grimme,[18] which has been recently implemented by some of us in QE.[19] The generalized-gradient approximation (GGA) and, in particular, the Perdew−Burke−Ernzerhof[20] (PBE) exchange−correlation

(11) Quintal, S. M. O.; Nogueira, H. I. S.; Félix, V.; Drew, M. G. B. *J. Chem. Soc., Dalton Trans.* **2002**, 4479–4487.

(12) (a) Nakamoto, K. *Infrared Spectra of Inorganic and Coordination Compounds*, J. Wiley and Sons: New York, NY, 1997; (b) Socrates, G. *Infrared and Raman Characteristic Group Frequencies*; J Wiley and Sons Ltd: Chichester, U.K., 2001; (c) V. Zelenak, V.; Vargova, Z.; Györyova, K. *Spectrochim. Acta, Part A* **2007**, *66*, 262–272.

(13) Briggs, D.; Seah, M. P. *Practical Surface Analysis*; J. Wiley and Sons: 1990.

(14) Shirley, A. *Phys. Rev. B: Solid State* **1972**, *5*, 4709.

(15) Moulder, J. F.; Stickle, W. F.; Sobol, P. E.; Bomben, K. D. *Handbook of X-Ray Photoelectron Spectroscopy*; Chastain, J. Ed.; Perkin-Elmer Corp.: Eden Prairie, MN, 1992.

(16) *NIST Standard Reference Database 20,* version 3.5, NIST: Gaithersburg, MD, **2007**; http://srdata.nist.gov/xps/.

(17) Baroni, S.; dal Corso, A.; de Gironcoli, S.; Giannozzi, P.; Cavazzoni, C.; Ballabio, G.; Scandolo, S.; Chiarotti, G.; Focher, P.; Pasquarello, A.; Laasonen, K.; Trave, A.; Car, R.; Marzari, N.; Kokalj, A. *Quantum ESPRESSO*, version; http://www.quantum-espresso.org/.

(18) Grimme, S. *J. Comput. Chem.* **2006**, *27*, 1787.

(19) Barone, V.; Casarin, M.; Forrer, D.; Pavone, M.; Sambi, M.; Vittadini, A. *J. Comput. Chem.* **2009**, *30*, 934.

(20) Perdew, J. P.; Burke, K.; Ernzerhof, M. *Phys. Rev. Lett.* **1996**, *77*, 3865.

Table 1. Crystal Data and Structure Refinement for **Zn1** and **Zn2**

	Zn1	Zn2
empirical formula	C48H32N8O16S8Zn4	C24H24N4O16Zn2
formula weight	1494.78	1510.48
temperature	293(2) K	293(2) K
wavelength	0.71073 Å	0.71073 Å
crystal system, space group	monoclinic, $P2(1)/c$	monoclinic, $P2(1)/c$
unit cell dimensions	a = 13.403(3)Å, α = 90°	a = 7.485(4)Å, α = 90°
	b = 12.843(3) Å, β = 96.30(3)°	b = 12.332(6) Å, β = 100.57(1)°
	c = 7.5005(15)Å, γ = 90°	c = 7.726(4)Å, γ = 90°
volume	1283.3(4) Å^3	691.9(6) Å^3
Z, calculated density	1, 1.934 Mg/m^3	1, 1.813 Mg/m^3
absorption coefficient	2.255 mm^{-1}	1.822 mm^{-1}
F(000)	752	384
crystal size	0.40 × 0.05 × 0.04 mm	0.20 × 0.20 × 0.08 mm
θ range for data collection	1.53−28.32°	2.77−28.35°
limiting indices	$-17 \le h \le 17$, $-9 \le k \le 17$, $-9 \le l \le 10$	$-7 \le h \le 9$, $-16 \le k \le 16$, $-9 \le l \le 10$
reflections collected/unique	8381/3170 [R(int) = 0.0875]	4321/1691 [R(int) = 0.0379]
completeness to θ	28.32°, 99.3%	28.35°, 98.0%
absorption correction	semiempirical from equivalents	semiempirical from equivalents
max. and min. transmission	0.9152 and 0.4657	0.8679 and 0.712
refinement method	full-matrix least-squares on F^2	full-matrix least-squares on F^2
data/restraints/parameters	3170/0/190	1691/2/112
goodness-of-fit on F^2	1.085	1.150
final R indices [$I > 2\sigma(I)$]	$R1$ = 0.0802, w$R2$ = 0.1797	$R1$ = 0.0357, w$R2$ = 0.1127
R indices (all data)	$R1$ = 0.1271, w$R2$ = 0.1990	$R1$ = 0.0463, w$R2$ = 0.1219
largest diff. peak and hole	1.149 and −1.494 e.A^{-3}	0.722 and −0.750 e.A^{-3}

functional have been adopted. A total of 12, 6, 6, 5, 4, and 1 valence electrons were explicitly considered for Zn, S, O, N, C, and H, respectively, while the interaction between the valence electrons and the ion cores was modeled by means of ultrasoft pseudopotentials.[21] The smooth part of the wave function was expanded in plane waves, with a kinetic energy cutoff of 30 Ry, while the cutoff for the augmented electron density charge was 250 Ry. The Brillouin zone integration was performed using the Monkhorst−Pack scheme,[22] with a 1 × 1 × 2 and 2 × 1 × 2 mesh for the **Zn1** and **Zn2** compounds, respectively. Both the cell constants and the internal parameters were fully optimized with a Broyden−Fletcher−Goldfarb−Shanno (BFGS) algorithm. Finite basis set effects were corrected following the procedure by Bernasconi et al.,[23] setting A = 40, E_0 = 30, and σ = 4 Ry. The convergence threshold for the residual atomic forces was 0.03 eV Å^{-1}, while the pressure tolerance in the cell optimization was 50 bar.

Results and Discussion

The structural and compositional features of **Zn1** and **Zn2** were extensively characterized by X-ray diffraction and by two different spectroscopic (XPS, FT-IR) methods. Remarkably, a similar reaction performed using the same amounts and molar ratios between the reactants and refluxing the suspension in water for 96 h instead of using hydrothermal conditions did not yield any new crystalline product. Instead the diffraction pattern of the obtained product reveals the presence of unreacted ligand. This proves the essential role played by hydrothermal conditions in driving the formation of the products. In fact, owing to the changes in the dielectric constant and viscosity of water, the increased temperature within a hydrothermal medium has a significant effect on the speciation, solubility, and transport of solids.[24] Furthemore, it should be pointed out that similar reactions with redox active species, such as Mn(II) and Cu(II), invariably leads to the oxidation of the thiol group to give disulfide, and, in the case of the reaction of $MnCl_2$ with the 2-mercaptonicotinic acid, the disulfide bridge formation was favored over the formation of Mn−S bond.[7b] In our study, the redox stability of Zn(II) was proved to play a key role in the formation of a coordination polymer since the ligand does not undergo oxidation and retains its integrity. This can also partially be ascribed to the higher affinity of Zn[8] for sulfur; this "thiophilicity" can be invoked to explain the stability of the ligand in these conditions, since the thiolate is expected to be less susceptible of oxidation when coordinated to a transition metal.

Description of the Crystal Structures. (Zn1). Zn1 (Figure 2a) crystallizes in a monoclinic setting, space group $P2_1/c$, with one zinc(II) cation and two 2-mercaptonicotinate in general position in the asymmetric unit. Both ligands are roughly flat (angles between the aromatic ring and the carboxylate group are about 15 and 30°) and exhibit a protonated nitrogen atom, deprotonated oxygen, and sulfur atoms, giving rise to a −1 charge, in accordance with the formulation and the charge balance. They both chelate the zinc cation through one oxygen and one sulfur atom, defining two ZnOCCCS six-member rings, with Zn−O and Zn−S distances lying in the usual range (see Supporting Information, Table 1SM for selected bond distances and angles), as shown in Figure 2a. A fifth oxygen atom, coming from a neighboring ligand, completes the coordination sphere of the zinc atom, which finally adopts a distorted square

(21) Vanderbilt, D. *Phys. Rev. B: Condens. Matter Mater. Phys.* **1990**, *41*, 7892.
(22) Monkhorst, H.; Pack, J. *Phys. Rev. B: Solid State* **1976**, *13*, 5188.
(23) Bernasconi, M.; Chiarotti, G. L.; Focher, P.; Scandolo, S.; Tosatti, E.; Parrinello, M. *J. Phys. Chem. Solids* **1995**, *56*, 501.
(24) (a) Hullinger, J. *Angew. Chem.* **1994**, *106*, 151. (b) Byrappa, K.; Haber, M. *Handbook of Hydrothermal Technology - Technology for Crystal Growth and Materials Processing*, William Andrews Publishing: Norwich, NY, 2001. (c) Sheets, W. C.; Mugnier, E.; Barnabé, A.; Marks, T. J.; Kenneth, R.; Poeppelmeier, K. R. *Chem. Mater.* **2006**, *18*, 7.

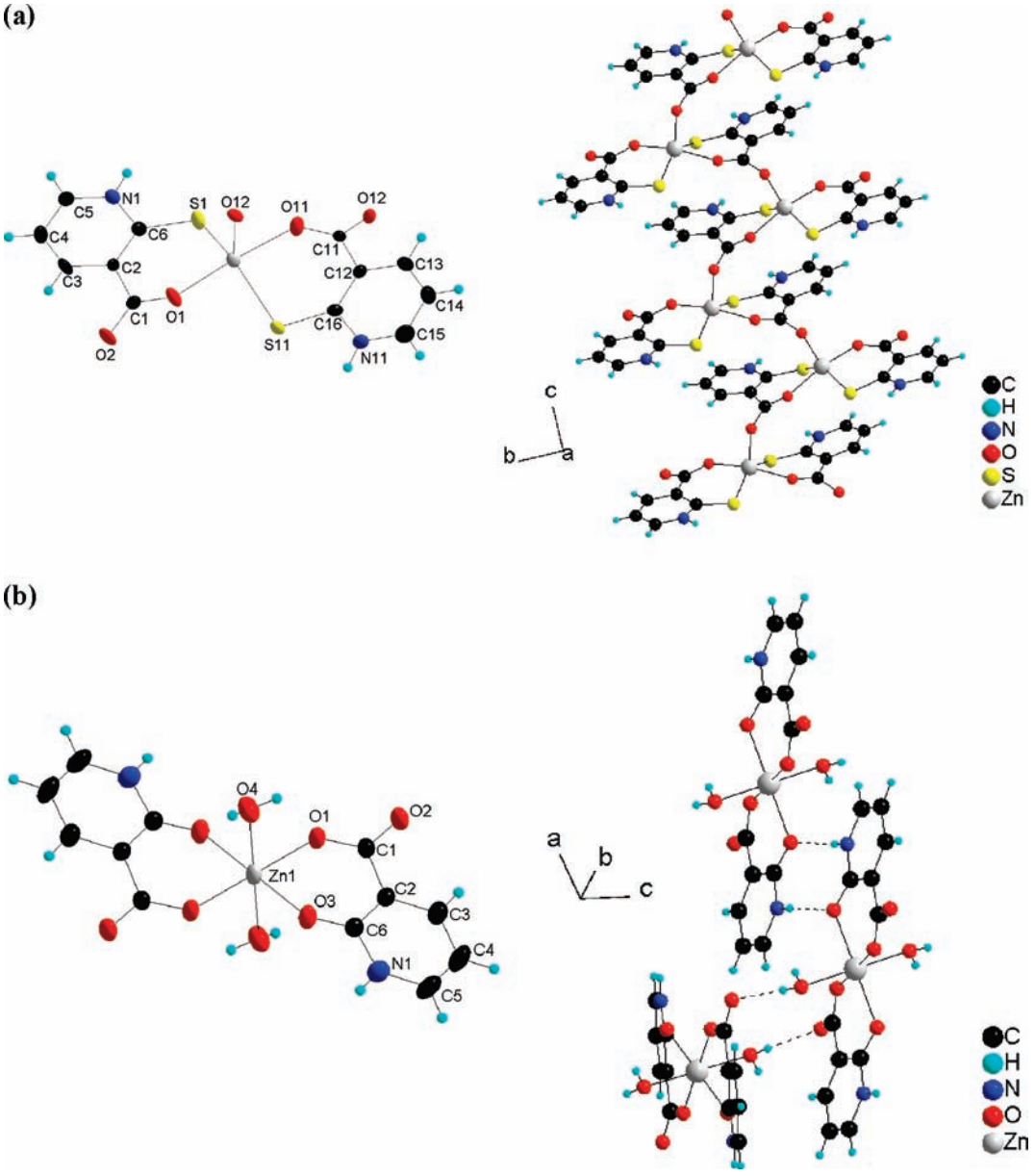

Figure 2. (a) Left: The **Zn1** complex; thermal ellipsoids are shown at the 50% probability level. Right: The one-dimensional polymeric chain running along the *c* axis. (b) Left: The **Zn2** complex; thermal ellipsoids are shown at the 50% probability level. Right: Hydrogen bonds (dotted lines) between the molecular complexes.

pyramidal environment. This finally defines polymeric chains of $Zn(C_6H_4NO_2S)_2$ running along the *c* axis (see Figure 2a, right). These chains interact weakly through N−H···O hydrogen bonds (N···O = 2.845 and 2.730 Å, N−H···O = 152.4 and 154.1°), defining finally a three-dimensional hydrogen-bonded network.

Before going on, it should be highlighted that, by reacting Zn acetate with the 6-mercaptonicotinic isomer, a completely different coordination fashion was achieved, characterized by the bifunctional ligand bridging of two different zinc atoms.[7a]

(**Zn2**). **Zn2** (Figure 2b) crystallizes in a monoclinic setting, space group $P2_1/c$, with one zinc(II) on the inversion center and one 2-hydroxynicotinate in general position in the asymmetric unit. Like in **Zn1**, the ligand is roughly flat (angle between the aromatic ring and the carboxylate group is about 15°) and exhibits a protonated nitrogen atom and deprotonated oxygen atoms, giving rise to a −1 charge, in accordance with the formulation and the charge balance. Each Zn cation is chelated by two symmetry-related ligands defining ZnOCCCO six-member rings, with Zn−O distances lying in the usual range (see Supporting Information, Table 2SM), and completes its coordination sphere by two symmetry-related water molecules. These 1:2 Zn:ligand complexes finally interact through N−H···O (N···O = 2.893 Å, N−H···O = 162.7°) and O−H···O (O···O = 2.722 and 2.796 Å, O−H···O = 168.7 and 162.0°) hydrogen bonds along the *a* axis and in the *b*,*c* plane respectively, defining a three-dimensional hydrogen-bonded network (Figure 2b). This compound is isostructural with its known Ni, Co, and Mn analogues.[25]

(25) (a) Wen, D. C.; Liu, S.-X. *Chin. J. Struct. Chem.* **2007**, *26*, 1281. (b) Zeng, M.-H.; Wu, M.-C.; Zhu, L.-H.; Liang, H.; Yang, X. W. *Chin. J. Chem.* **2007**, *25*, 16. (c) Li, Y.-M.; Che, Y.-X.; Zheng, J.-M. *Chin. J. Struct. Chem.* **2006**, *25*, 572.

Both compounds (**Zn1** and **Zn2**) were prepared using the same experimental conditions. Although they present rough similarities (1:2 Zn:ligand stoichiometry, coordination mode of the ligands), they also exhibit differences both at the local and global scale. The Zn cation is five-coordinated and lies out of the plane defined by the coordinating atoms of the ligands in **Zn1**, whereas it is 6-coordinated and lies in this plane in **Zn2**; one-dimensional polymeric chains are present in **Zn1**, whereas only isolated molecular complexes form **Zn2**. It is nevertheless difficult to conclude if these differences are related to the nature of the ligands or are just serendipitous.

XPS Analysis. As pointed out by the X-ray crystal structure, the Zn atom in the compound **Zn1** is coordinated by both sulfur and oxygen atoms. X-ray data were then complemented with the outcomes of XPS measurements to eventually confirm the chemical environment and the oxidation states of different species (Zn, S, O, and N) in **Zn1** and **Zn2**. In Table 2, the binding energies (BE) of $Zn2p_{3/2}$, S2p, O1s, and N1s core levels in **Zn1** and **Zn2** and in the free 2-mercaptonicotinic acid are reported.

As far as zinc is concerned, the BE of the $Zn2p_{3/2}$ region in **Zn1** has a BE of 1021.1 eV, which is lower than the BE reported for ZnS (1021.7−1022.0 eV) and more similar to those of ZnO (1021.1−1022.4 eV).[15,16]

In Figure 3, the Zn2p region of zinc in **Zn1** is shown, which displays the two components of the doublet due to the spin−orbit coupling. The Zn α parameter, determined as reported in literature,[26] resulted to be 2009.9 eV. This value is intermediate between those of the Zn in ZnO (2009.5−2010.2 eV) and the values reported for ZnS (2010.3−2011.7 eV)[27] and in agreement with an "intermediate" state for the zinc atom, bonded to both oxgen and sulfur atoms, as shown by the X-ray crystal structure.

Upon coordination of the zinc ion, both the S2s and S2p regions slightly shift to a higher BE with respect to the 2-mercaptonicotinic acid, passing from 226.0 to 226.2 eV and from 161.8 to 162.3 eV, respectively.[15,16,27] The experimentally detected values are in good agreement with those reported for sulfur in ZnS, 226.3 and 162.2−162.4 eV for S2s and S2p, respectively. Conversely, the nitrogen N1s peak is not shifted, although the protonation observed in the crystal structure, and retains the same value of BE, i.e. 400.2 eV. This value, which is higher than the one reported for nitrogen in pyridine (399.0 − 399.3 eV),[28] can be ascribed to the presence of the carboxylic and thiol moieties on the pyridinic ring, which could lead, the former to the formation of the zwitterionic form of the mercaptonicotinic acid, and the latter to the protonation of the nitrogen by the thiol groups. Both events, causing the protonation of the nitrogen atom, would explain the higher BE observed. In this case, it is particularly evident as the availability of the X-ray structure allows to confirm and strengthen the XPS values assignments.

For complex **Zn2**, the BE of $Zn2p_{3/2}$ is 1021.9 eV, a value very close to the one reported for ZnO in literature.[13,15,16] The Zn2p doublet of **Zn2** is reported in the Supporting Information, Figure 1SM.

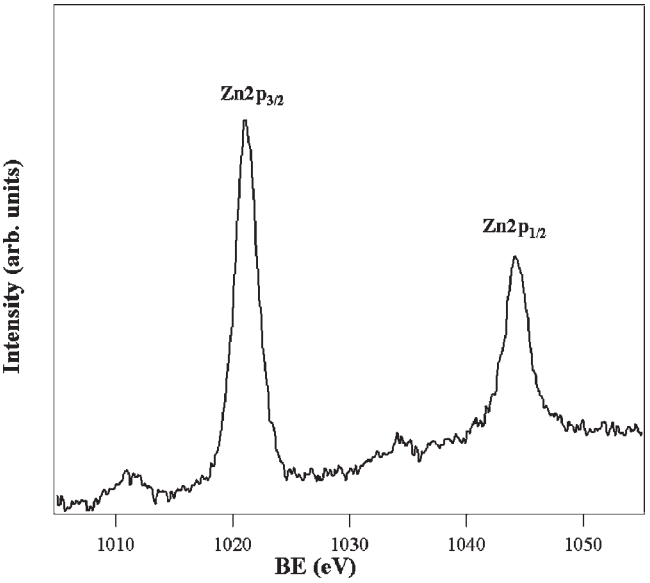

Figure 3. Zn2p region of the complex **Zn1** (BE values are corrected for charging effects).

Table 2. BE Values (Corrected for Charging Effects) of the Different Elements

sample	O1s (eV)	S2p (eV)	S2s (eV)	N1s (eV)	$Zn2p_{3/2}$ (eV)
2-mercaptonicotinic acid	532.2	161.8	226.0	400.2	−
Zn1	531.0	162.3	226.2	400.2	1021.1
Zn2	531.2 532.0 532.5	−	−	400.4	1021.9

The experimental Zn α parameter in **Zn2** is 2009.0 eV, and this value corresponds to zinc in ZnO, in agreement with the fact, evidenced by X-ray structure, that the zinc atom is coordinated by two oxygen atoms.[13,14]

C1s region was deconvolved in four components, peaked at 284.6 (adventitious carbon), 285.4, 286.3, and 288.4 eV (Supporting Information, Figure 2SM). Whereas the first one is the adventitious carbon, the last three values are attribuable to carbon atoms present in the ligand in different chemical environments. On the basis of the different electronegativities of the heteroatoms in the ligand, the peak at 288.4 eV corresponds to the carboxylic carbon, the α- and β-carbon atoms have a signal peak at 286.3 eV, whereas the peak at 285.5 eV can be ascribed to carbon atoms of the pyridine ring.[15,16]

The O1s peak (Supporting Information, Figure 3SM) was deconvolved in three different components at 531.2, 532.0, and 532.5 eV. The first two peaks at lower BE's are attribuable to the oxygen atoms of the ligand coordinated to the metal center. The one at a higher BE derives from contaminants.

N 1s is peaked at 400.4 eV, nearly the same value found for **Zn1**. This confirms that it is a protonated nitrogen, as supported by XRD analysis. Also in this case, an unambiguous assignment was possible on the basis of the X-ray structure available.

FT-IR analysis. Complexes **Zn1** and **Zn2** were further characterized by FT-IR spectroscopy.

(26) (a) Wagner, C. D. *Faraday Discuss. Chem. Soc.* **1975**, *60*, 291. (b) Wagner, C. D. *Anal. Chem.* **1975**, *47*, 1201.

(27) Wong, J. W. L.; Sun, W. D.; Ma, Z. H.; Sou, I. K. *J. Electron. Spectrosc. Relat Phenom.* **2001**, *113*, 215.

(28) (a) Pietrzak, R.; Wachowska, H.; Nowicki, P. *Energy Fuels* **2006**, *20*, 1275. (b) Lahaye, J.; Nanse, G.; Bagreev, A.; Strelko, V. *Carbon* **1999**, *37*, 585.

In this case, the aim of the analysis was to investigate the changes induced by the coordination to the metal atom on the wavenumbers of the main bands characterizing the two ligands and to relate these shifts to their peculiar coordination fashions. As already observed in the discussion of XPS data, also in this case, the assignment of the IR bands was driven and supported by the available X-ray data.

The spectra of **Zn1** and of the unreacted 2-mercaptonicotinic acid are comparatively superimposed in Figure 4, where the main vibrational bands are also attributed.

In the low wavenumber region, the band at 408 cm^{-1} was ascribed to the Zn−O stretching bonded to the carboxylate.[12]

The weak features at 752 and 709 cm^{-1} [12] were ascribed to the C−H and C−C bending of the aromatic ring. These bands were also present in the spectrum of the ligand. The weak thioamide bands (IV and III)[12b,37] were present at 642 and 1058 cm^{-1}, respectively. In 2-mercaptonicotinic acid, the IV thioamide band is peaked at 1074 cm^{-1}.[29] This shift can be ascribed to the coordination of sulfur to zinc, as pointed out by the X-ray structural determination.

The other two characteristic thioamide bands (I and II) were detected at 1569 and 1356 cm^{-1}.[12b,37]

At 1612 and at 1487 cm^{-1} the COO^- asymmetric and symmetric stretching vibrations were evidenced. Although this region of the spectrum presents many vibrational features, whose unambiguous assignment is not straightforward, we tentatively assigned these two bands, on the basis of literature reference values,[12a−c] to the carboxylate stretching.

The $\Delta\nu$ ($COO^-\nu_{as} - COO^-\nu_{sym}$) = 125 cm^{-1} indicated that the carboxylate bound the metal in a bridging way,[12a−c] as supported by XRD analysis. This value is, as expected,[12a−c] lower than the value of the corresponding sodium salt; in fact, the sodium salt of 2-mercaptonicotinic acid gave a value of 165 cm^{-1}.[37]

The weak stretching band of S−H at 2412 cm^{-1}, present in the unreacted ligand spectrum, disappears in the **Zn1** spectrum, as a consequence of the deprotonation. At 3440 cm^{-1}, a broad and weak band in the coordination polymer was ascribed to the N−H stretching vibration due to the protonated pyridinic nitrogen, as confirmed by XRD and XPS analysis. In the ligand spectrum, this band is weaker because of the tautomeric equilibrium between the thiol and the thionic forms of 2-mercaptonicotinic acid.

All the changes observed in the IR spectra of the coordination compounds investigated here can be used as guidance values to investigate other complexes based on similar ligands, in the case where the X-ray crystal structure is not available.

As far as the FT-IR spectrum of compound **Zn2** is concerned (Supporting Information, Figure 4SM, and also see values in the Experimental Section), at 3371 cm^{-1} the stretching of N−H in the pyridine ring of the ligand is well visible.

The band at 3222 cm^{-1} present in 2-hydroxynicotinic acid is instead absent in the spectrum of the complex due to the coordination of the oxygen, from the OH group, to the metal. Coordinated water molecules in the apical positions of the complex are responsible for the broad band centered at 3000 cm^{-1}.

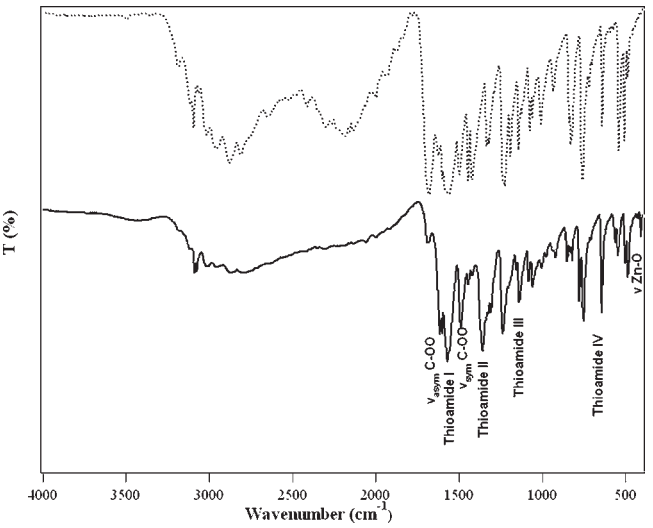

Figure 4. FT-IR spectra of 2 mercaptonicotinic acid (dashed line) and **Zn1**.

Concerning the carboxylate group, the $\Delta\nu$ ($COO^-\nu_{as} - COO^-\nu_{sym}$) = 85 cm^{-1} suggests a chelating bidentate coordination of the ligand to the metal center, as supported by XRD analysis. The amide II band is present at 1572 cm^{-1}. Other amide bands are present at 1234 and 573 cm^{-1}.[12b]

At 404 cm^{-1} the band relative to Zn−O stretching is visible.[12]

Thermal Behavior and Decomposition Pattern of the Two Compounds. These Zn-based complexes with 2-mercaptonicotinate and 2-hydroxynicotinate are also interesting compounds as potential single-source precursors for the one-step synthesis (through controlled calcination) of nanostrutured ZnO_xS_y ($0 \le x, y \le 1$).

To investigate the decomposition pattern and the products of the two compounds, thermogravimetric measurements were performed in air and nitrogen atmospheres, from 30 to 800 °C for **Zn1** and in air only for **Zn2**. In the Supporting Information, Figure 5SM, the two TGA curves for **Zn1** are shown.

As it can be seen in the Supporting Information, Figure 5SM, the compound presents a clear decomposition pattern consisting of different steps. Thermal decomposition starts in air in the thermal range of 200−300 °C, and a weight loss of 41% was detected.

From 300 °C up to 423 °C, a further loss of 13% was detected. From 420 to 605 °C two further losses of 16% and 13% respectively, were observed. A last decomposition step was observed from 420 °C up to 600 °C. The polymeric nature of **Zn1** must be taken into account to justify the presence of multiple-weight losses. In fact, the simple complex $Zn(C_6H4NO_2S)_2$, obtained by precipitation from the zinc salt, decomposes to ZnO in a single step path.[34]

In a nitrogen atmosphere, the decomposition path is, of course, different, and it occurs in three different thermal ranges: 250−300, 300−350, and 350−400 °C.

In these conditions, at 800 °C the residual mass was 25.7% in agreement with the formation of ZnS.

(29) Yang, Q.; Chen, S.; Gao, S. *J. Therm. Anal. Calorim.* **2007**, *90*, 881–885.

Complex **Zn2** exhibits a four-step decomposition path in air (see Supporting Information, Figure 6SM). The first one is between 100 °C up to 200 °C and corresponds to the loss of the water molecules present in the complex. A second loss is in the range of 200−400 °C, and it is ascribable to thermolysis of the ligand. The other two steps are comprised between 400 and 500 °C with a remaining weight of 21.8%, corresponding to the final formation of ZnO.

The formation of ZnS and ZnO in the case of **Zn1** and **Zn2**, respectively, proves that the two complexes could be used as single-source molecular precursors for the formation of nanostructured ZnS and ZnO. However, the actual nanostructure of the resulting materials should be assessed, and at this regard, investigation on the thermal decomposition of significant amounts of the two compounds are currently in progress.

DFT Calculations: Structure and Stability. The stability of the complexes was also studied by DFT calculations. We considered not only the **Zn1** and **Zn2** compounds but also their unknown analogues, i.e., the hydrated derivative of **Zn1**, isostructural with **Zn2** and hereafter indicated **Zn1-hyd**, and the dehydrated derivative of **Zn2**, isostructural with **Zn1** and hereafter indicated as **Zn2-dry**). The theoretical cell constants (see Table 3) fairly agree with the experimental ones, the largest (but still acceptable) deviations being found for c (−3% and −5% for **Zn1** and **Zn2**, respectively).

A similar result has been already found previously[30] and is due to the overestimation of the dispersion interaction obtained when the Grimme parametrization is used in solid systems. A good agreement between theory and experiment is also found as far as internal parameters are concerned (see Supporting Information, Tables 1SM and 2SM). This validates our calculations, justifying their use in the discussion below.

From a qualitative point of view, noncovalent interactions seem to favor the hydrated form for the hydroxynicotinic complex, whereas the opposite is true for the mercaptonicotinic complex. In fact, replacing the hydroxynicotinic ligands of **Zn2** by mercaptonicotinic ligands, as in **Zn1-hyd**, implies that the N−H···O hydrogen bonds are turned into the substantially weaker N−H···S interactions. In contrast to that, no significant differences can be found in the interactions occurring in the **Zn1** and **Zn2-dry** compounds.

It can be interesting to consider hydration/dehydration process, which could convert **Zn1** into **Zn1-hyd** and **Zn2** into **Zn2-dry**. This can be done with the so-called atomistic thermodynamics, where the information derived by DFT total energies is employed to compute thermodynamic potential functions.[31] In synthesis, we consider the process:

$$\mathbf{X}(s) + 2H_2O(g) \rightarrow \mathbf{X}(H_2O)_2(s) \quad (1)$$

where **X** and $\mathbf{X}(H_2O)_2$ are the anhydrous and hydrated forms of the hydroxy−mercapto−nicotinate complexes, respectively. At given (T,p) conditions, the equilibrium of eq 1 is fixed by the Gibbs energy, defined as

$$\Delta G(T, p_{\mathbf{X}(H_2O)_2}, p_x, p_{H_2O}) = g_{\mathbf{X}(H_2O)_2}(T, p_{\mathbf{X}(H_2O)_2}) - g_{\mathbf{X}}(T, p_{\mathbf{X}}) - 2\mu_{H_2O}(T, p_{H_2O}) \quad (2)$$

For practical purposes, we can neglect the solid/gas equilibrium of the complexes as well as the entropy differences between them. We note that the latter assumption implies that the entropic contribution by the vibrations of the lattice-included water molecules is negligible. This approximation is, in general, quite acceptable at RT.[32] Under the above enumerated assumptions, the molar free energies of the condensed phases can be replaced by the DFT total energies:

$$\Delta G(T, p_{H_2O}) = E_{\mathbf{X}(H_2O)_2} - E_{\mathbf{X}} - 2\mu_{H_2O}(T, p_{H_2O}) \quad (3)$$

Furthermore, we estimate $\mu_{H_2O}(T, p_{H_2O})$ as follows:

$$\mu_{H_2O}(T, p_{H_2O}) = E_{H_2O} + \tilde{\mu}_{H_2O}(T, p^0) + k_B T \ln\left(\frac{p_{H_2O}}{p^0}\right) \quad (4)$$

where E_{H_2O} is the DFT total energy of a water molecule computed in a large supercell, while $\tilde{\mu}_{H_2O}(T, p^0)$ includes contributions from the rotations and the vibrations of the molecules as well as the entropy of the ideal gas at $p^0 = 1$ atm, and can be obtained from tabulated data.[33]

On applying eq 3 at $T = 300$ K, we compute that the hydrated form of the mercaptonicotinic complex is unfavored with respect to the dehydrated form **Zn1** even at a $p_{H_2O} = 1$ atm, whereas at the same temperature the hydroxynicotinic complex **Zn2** is stable against dehydration for water partial pressures as low as 10^{-6} atm. Even at 400 K, water partial pressures lower than 10^{-2} atm are needed to dehydrate **Zn2**. This is quite compatible with the above discussed TGA results, showing that the loss of water molecules occurs between 100 and 200 °C.

Electronic Structure. The electronic density of states (DOS) of **Zn1** and **Zn2** compounds, computed by applying a 0.27 eV Gaussian broadening to the DFT monoelectronic levels, are reported in Figure 5. The Löwdin population analysis has been carried out to obtain the local density of states (LDOS) curves relative to the Zn and S atoms and to the H_2O molecules.

The main difference between **Zn1** and **Zn2** is that in the former the top of the valence band is composed, as expected, by sulfur lone pairs, whereas in the case of

Table 3. Theoretical Unit Cell Parameters for the Examined Compounds[a]

	a (Å)	b (Å)	c (Å)	β (°)
Zn1	13.100 (−2.3%)	12.829 (+0.1%)	7.278 (−3.0%)	93.9
Zn1-hyd	8.615	12.466	7.268	103.0
Zn2	7.554 (+0.9%)	12.224 (−0.8%)	7.244 (−5.0%)	102.3
Zn2-dry	12.495	12.393	7.476	93.5

[a] See text. Deviations from experimental values (see Supporting Information, Tables 1SM and 2SM) are indicated in parentheses.

(30) Bencini, A.; Casarin, M.; Forrer, D.; Franco, L.; Garau, F.; Masciocchi, N.; Pandolfo, L.; Pettinari, C.; Ruzzi, M.; Vittadini, A. *Inorg. Chem.* **2009**, *48*, 4044.

(31) Reuter, K.; Stampfl, C.; Scheffler, M. Ab Initio Thermodynamics and Statistical Mechanics of Surface Properties and Functions. In *Handbook of Materials Modeling, Part A. Methods*; Yip, S. Ed.; Springer, Berlin, Germany, 2005.

(32) Law, J. T. *J. Phys. Chem.* **1955**, *59*, 67.

(33) NIST-JANAF Thermochemical Tables, Fourth edition, *J. Phys. Chem. Ref. Data*, Monograph 9; 1998

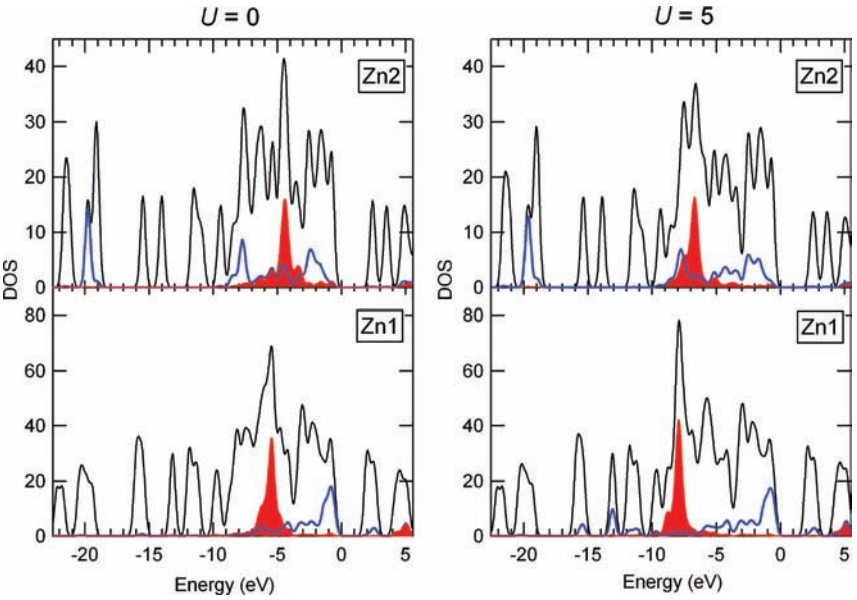

Figure 5. DOS curves of **Zn2** and **Zn1** compounds. Relevant LDOS curves are also shown: red-filled regions are Zn states, while blue-solid curves are sulfur and water LDOS in **Zn1** and **Zn2**, respectively. Electronic energies are referred to the valence band edge, so that only states with $E < 0$ are occupied. Left panel: GGA calculations; right panel: GGA+U calculations with $U = 5$ eV.

Zn2, it is composed by oxygen lone pairs. This has dramatic consequences on the band gap, which, in the case of **Zn1**, turns out to be narrower by ~0.5 eV. The bottom of the conduction band is essentially composed by ring π^* combinations in both cases. A well-known shortcoming of the application of currently available GGA functionals to zinc compounds concerns the underestimation of the binding energy of the semicore Zn3d levels. This gives rise to spurious interactions and to an artificial reduction of the band gap. A way to circumvent this problem is provided by the so-called GGA+U approach,[34] which consists in the application of a Hubbard U term.[35] The values of the U parameter are not only sensitive to the treated systems but also to the computational details, such as the adopted pseudopotentials, and should be determined from a self-consistent procedure based on the linear-response theory.[36] In the present case, we simply used $U = 5$ eV, which is a typical value adopted in many GGA+U calculations, and seemed to fit rather well the XPS experiments (see below). We emphasize that the effects of the GGA+U approach on the thermodynamical aspects, discussed above, is negligible. The GGA+U computed DOS curves are shown in Figure 4, right: the main Zn3d peaks of the **Zn1** and **Zn2** compounds are shifted toward higher binding energies by ~2.5 eV, and their shapes become more similar.

On the basis of the GGA+U results, *theoretical* valence band photoemission spectra were obtained by computing weighted density of states (WDOS) curves. This was made by weighting the GGA+U levels by the photoionization cross sections and using tabulated data for the atomic subshell cross sections.[37] A 0.7 eV Gaussian broadening has been adopted in order to match the resolution of the experiment.

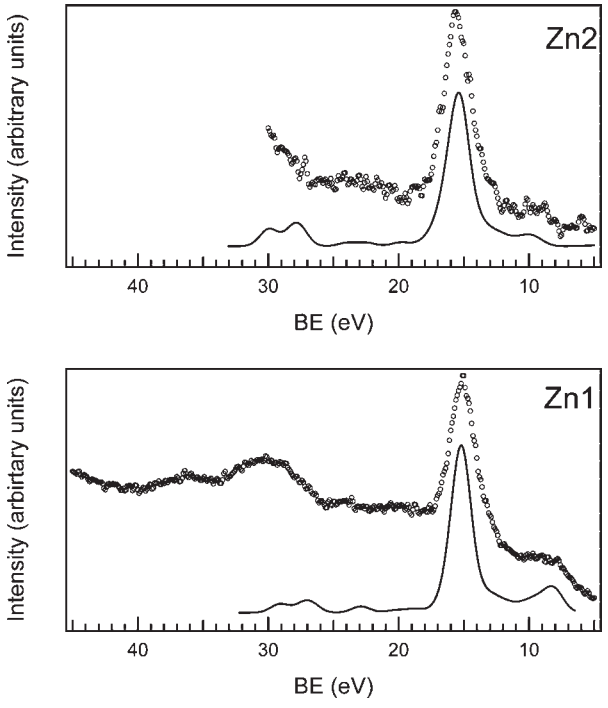

Figure 6. Valence XPS regions (circles) compared with theoretical WDOS curves (see text, solid lines) for (top) **Zn2** and (bottom) **Zn1** compounds. The WDOS curves have been obtained from the GGA+U eigenvalues, applying a 0.7 eV Gaussian broadening. The energy scales of the WDOS curves have been shifted to align the maxima of the main peaks.

The WDOS curve and the Al Kα XPS spectrum of **Zn1** are compared in Figure 6 (bottom). Both curves show a prominent peak, used to align the theoretical and the experimental curves, ascribed to the emission from the Zn3d states on the basis of the Löwdin population analysis. Theoretical calculations also allow to assign

(34) Karazhanov, S. Z.; Ravindran, P.; Kjekshus, A.; Fjellvag, H.; Grossner, U; Svensson, B. G. *J. Appl. Phys.* **2006**, *100*, 043709.
(35) Anisimov, V. I.; Zaanen, J.; Andersen, O. K. *Phys. Rev. B: Condens. Matter Mater. Phys.* **1991**, *44*, 943.
(36) Kulik, H. J.; Cococcioni, M.; Scherlis, D. A.; Marzari, N. *Phys. Rev. Lett.* **2006**, *97*, 103001.
(37) Yeh, J.; Lindau, I. *At. Data Nucl. Data Tables* **1985**, *32*, 1.

the weak peak which marks the onset of the photoemission of **Zn1** at about 8 eV, and is absent in **Zn2** (Figure 6), to the ionization from the sulfur lone pair levels. Accordingly, the band gap is computed to be narrower on passing from **Zn2** to **Zn1** (2.50 vs 2.19 eV).

Conclusions

By hydrothermal reaction of 2-mercaptonicotinic and 2-hydroxynicotinic acids with Zn acetate, two different crystalline complexes were obtained, which, although the similarities between the two ligands, are characterized by different structures and coordination modes around the central metal atom.

In particular, as evidenced by single-crystal X-ray determination, both **Zn1** and **Zn2** structures crystallize in a monoclinic setting, and in both structures, the two ligands are roughly flat. In the case of **Zn1**, the two ligands chelate the zinc cation through one oxygen and one sulfur atom, defining two ZnOCCCS six-member rings, with Zn−O and Zn−S distances lying in the usual range. As far as **Zn2** is concerned, each Zn cation is chelated by two symmetry-related ligands defining ZnOCCCO six-member rings, with Zn−O distances lying in the usual range. Moving from **Zn1** to **Zn2**, two important differences are present: (i) the Zn cation is five-coordinated and lies out of the plane, defined by the coordinating atoms of the ligands in **Zn1**, whereas it is six-coordinated and lies in this plane in **Zn2**; (ii) one-dimensional polymeric chains are present in **Zn1**, whereas only isolated molecular complexes form **Zn2**.

The chemical environment of the present species was investigated by XPS, yielding the core level binding energies for the two different O−Zn−O and S−Zn−O coordination situations.

Theoretical outcomes, in very good agreement with XPS data, provide insight into the differences between **Zn1** and **Zn2**, including structure, stability, and electronic properties.

Finally, as evidenced by TGA analyses, the formation of ZnS and ZnO in the case of **Zn1** and **Zn2**, respectively, proves that the two complexes could be used as single-source molecular precursors for the formation of nanostructured ZnS and ZnO.

Acknowledgment. The European Union and the Program Short Term Mobility of the Italian National Research Council (CNR) are gratefully acknowledged for financially supporting a research stay of S.G. at the Institute Lavoisier, Versailles (France). The University of Padova, the Italian National Research Council (CNR), the Italian Consortium INSTM, and CNRS are acknowledged for providing money and equipment. The Laboratorio Interdipartimentale di Chimica Computazionale (LICC) of the Università di Padova is acknowledged for support of the computer facilities. The authors thank Mrs. Roberta Saini for TGA-DSC analyses and Mr. Antonio Ravazzolo for his skillful technical support.

Supporting Information Available: BE curves, FT-IR spectra of 2-hydroxynicotinic acid and **Zn2**, thermogravimetric curves, and selected bond lengths and angles of **Zn1** and **Zn2**. This material is available free of charge via the Internet at http://pubs.acs.org.